

## The Evaluation of SfM Technique in the Determination of Surface Deformation on Skidding Roads Following Timber Harvesting

Sercan Gülci\*<sup>ID</sup>, Seçkin Şireli<sup>ID</sup>

Kahramanmaraş Sütçü İmam University, Faculty of Forestry, 46040 Kahramanmaraş, Turkey

### Abstract

Forest roads are necessary engineering structures for accessing and managing forestry resources. Considering the difficult terrain and its numerous variable effects, it must be ensured that the capacity of forest roads function adequately and that the road platform is suitable for vehicle traffic. This study aimed to focus on the determination and evaluation of deformation on the surface of the soil roads in the forest using SfM (Structure from Motion) technique. The study focused on the usage opportunity of close-range photogrammetry in the analysis of surface deformation on skidding roads used for forestry operations. Field surveys were conducted on a newly constructed skidding road for forestry operations with a four-wheel farm tractor. The geo-spatial location of the road was obtained by a Total Station (TS) prior to harvesting operation. A digital camera mounted on a 3.5 m high pole was used as a carrier platform in the field survey. The photographs with front and side overlaps (approximately 60% and -80%) were obtained from 95 m segment of the unpaved road. The spatial (X, Y and Z) differences between field measurements- and SfM-based models were compared using Root Mean Square Error (RMSE), and the values of spatial error (SfMXY: 0.048; SfMZ: 0.010 for estimated model) were calculated. The change rate of stable, accumulations and abrasions on the road surface were calculated as 0.165%, 48.642% and 51.192%, respectively. The present study demonstrated that the use of semi-automatic measurement technique offers a promising potential for the evaluation of forest road surface deformation.

**Keywords:** Forest roads, Surface degradation, Point cloud, SfM, Close-range photogrammetry

### 1. Introduction

In Turkey, forest operations have recently involve greater amount of mechanization in timber production process, which can be listed as one of the primary goals in the sector (Erdaş et al., 2014). However, mechanized harvesting activities can result in ecological damages (i.e. residual stand damage, soil disturbance etc.) at stand scale level (Worrell and Hampson, 1997; Akay et al., 2007; Öztürk et al., 2017). Besides, the forest roads which provide access to forests during mechanized harvesting activities may cause crucial impact on stand structures if they are not planned appropriately (Arıcak and Acar, 2008; Demir, 2012).

Forest roads, which have so far been extensively studied in terms of economic, ecological, aesthetic and ergonomic point of view, are necessary facilities for implementing forestry activities in a forest enterprise. In general, direct observation methods such as land observation and evaluation and the analysis of technical, ecological, aesthetic and environmental factors for road planning are widely used in the determination of quality standards and existing conditions for forest roads (Eroğlu

et al., 2003; Ünver, 2013; Çankal, 2016; Arıcak and Genç, 2018). Surface deformations and abrasions on structures with a coated surface such as roads were measured based on specialists' observations until the 1980s. On the other hand, today's technology allows carrying out a more rapid road surface deformation measurement thanks to electronic sensors such as digital video cameras and laser sensors that can be mounted on a land vehicle or pole (İnan and Öztürk, 2016; Akgül et al., 2017; Hrûza et al., 2018).

Terrestrial measurements used to analyze structure surfaces involve various labor intensive processes. Therefore, sensors which can be mounted on a carrier platform with different properties are usually preferred. High resolution data obtained from carrier platforms such as air vehicles and satellites are particularly used for this purpose. However, areal measurement techniques may pose some difficulties in terms of time, cost and safety in various situations (Schnebele et al., 2015; Zhang et al., 2016). Besides, they cannot be widely used due to flight problems of areal measurement devices as well as a high and dense canopy cover.

\*Corresponding author: Tel: +90 344 300 1749 E-mail: [sgulci@ksu.edu.tr](mailto:sgulci@ksu.edu.tr)

Received 02 Aug 2019; Accepted 19 Aug 2019

This work is licensed under a Creative Commons Attribution-NonCommercial 4.0 International License



Nowadays, photogrammetry technique and technology provide operators and researchers with an effective tool for effective data collection. Thanks to the development of “Structure from motion” (SfM) technique and images obtained from digital cameras, 3D surface models can be easily generated. SfM technique is widely preferred by researchers and operators because it offers highly accurate, low-cost and rapid surface model generation (Micheletti et al., 2015). Therefore, more and more commercial or open source SfM based software products have been developed and used in today’s marketplace. Existing programs do not significantly differ from each other in terms of 3D point cloud generation performance and accuracy (Pierzchała et al., 2016). The SfM technique can produce successful models with reasonable accuracy on a variety of complex surfaces compared to terrestrial laser scanning systems (Seki et al., 2017; Akay et al., 2018; Şireli, 2019; Yurtseven et al., 2019).

Recent studies on LIDAR and SfM based analysis of road surface deformation have demonstrated that SfM technique can generate data at centime sensitivity for surface deformation models (Akay, 2016; Seki et al., 2017; Hrůza et al., 2018; Şireli, 2019). Because road surface performance and deformation measurements offer great advantages for operators and researchers, automatic techniques are widely used

instead of manual methods (Ahmed et al., 2011). Using close range photogrammetry, this study aimed to evaluate road surface deformation and abrasion following whole-tree extraction from stump sites on a new skidding road. SfM technique was used along with a digital camera mounted on a specially designed pole in order to model the surface of skidding road. Benefiting from remote sensing and Geographic information system (GIS), the present study aimed to offer tangible data and set the basis for scientific research on the development of temporal deformation models for forest roads.

## 2. Material and Methods

### 2.1. Study Area

Compartment 33 located in Başkonuş Forest Enterprise Chief within the border of Kahramanmaraş Forest Regional Directorate was selected as the study area. The dominant tree species in this area is Buritian pine (*Pinus brutia* Ten.). The geographical location of the study area is 37°35’17.64” and 36°36’15.35” N and 37°35’17.09”-36°36’11.74” E (GDF, 2012). A new skidding road was built in the study area for logging process using whole-tree method which lasted for three months. A four-wheel farm tractor was used for skidding operations (Figure 1).

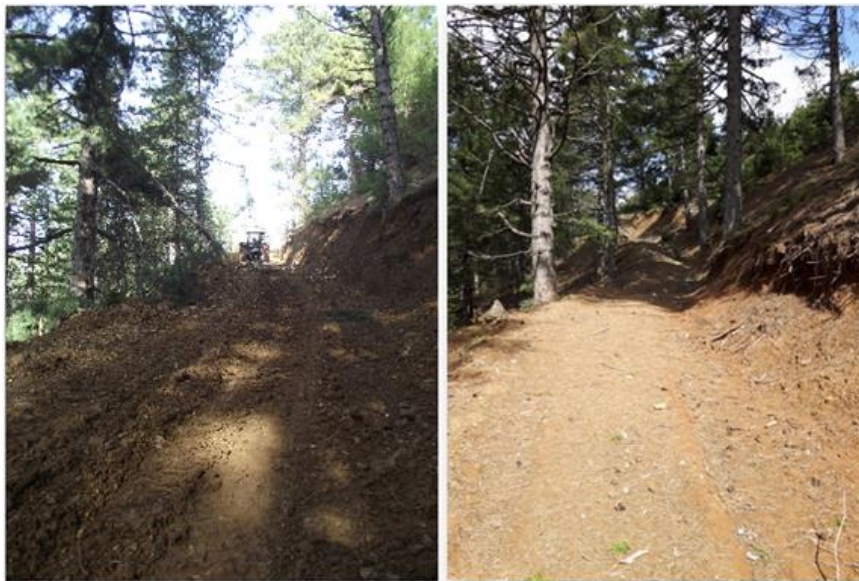


Figure 1. Descriptive photos taken in the study area on different days

### 2.2. Equipment

GNSS-GPS, Total Station (TS), a pole (ground carrier platform for sensor), Ground Control Point (GCP) targets, a digital camera and a steel tape measure (20 m) were used in the field studies. GCP targets were designed as cardboard materials at a dimension of A3 (297 x 420 mm) in order to obtain spatial data. A pole was used to mount digital camera.

This pole was made from aluminum material (0.5 cm width) and divided into three pieces (1.25 m + 1.25 m + 1.00 m) for easy carriage. Agisoft PhotoScan, which is a

widely used software for image processing, was preferred due to its integration into SfM technique. PhotoScan software, which has a user-friendly interface, allows classifying spatial (X-Y-Z) 3D point clouds thanks to SfM and Multi-View Stereo (MVS) algorithms. In addition, it enables users to define different parameters during image processing (Agisoft, 2016). WGS84 UTM Zone 37N projection system was used in GIS analysis run in ArcGIS software (Esri, 2011).

A TS (LEICA TCR407) and a GNSS-GPS (Macellan SPECTRA PRECISION SP-80) were used for geographical measurements. Total of 20 GCPs in red, white and green were used for ground truthing. A Sony DSC-HX400V 20.4 MP digital camera with an internal GPS module was used during digital image collection. PlayMemories software, which can be downloaded on Android smartphones, was used for image capturing with the digital camera.

### 2.3. Field Studies

The digital camera mounted on the pole which was designed as a ground platform was used to capture overlay images of the road surface. The angle closest to the nadir was determined by trial and error method (Figure 2). Cylindrical and spherical levels on the digital camera holder were vertically and horizontally adjusted. The images were captured after the horizontal stability of the digital camera was adjusted at a low angle in proportion to the ground (Figure 2b; 3). The images were captured every two meters for a side and forward overlay ratio of at least 60% and 80%, respectively.

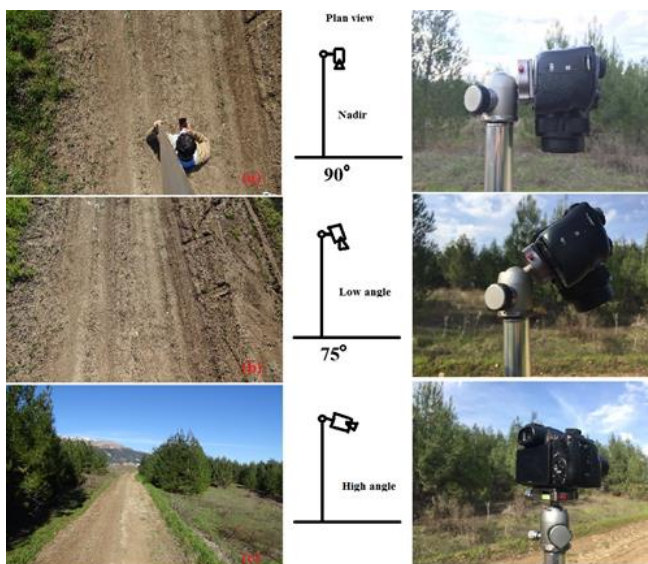


Figure 2. The position of the digital camera mounted on the pole in proportion to road surface and sample images (a: Nadir, b: Low angle, c: High angle)

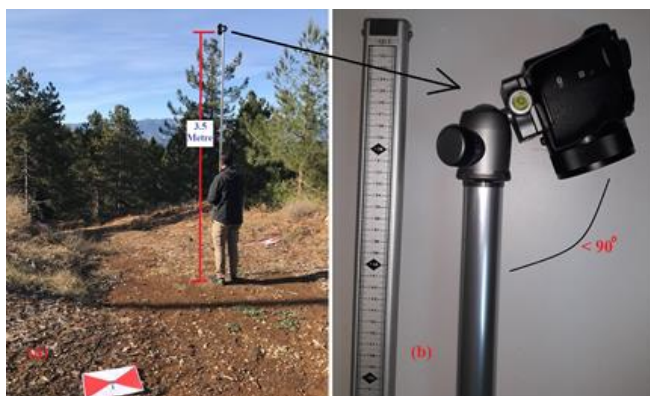


Figure 3. Position of the pole and camera in image capturing (a: The pole - sensor carrier platform, b: the positioning of the digital camera on the pole at a low angle)

For a more sensitive SfM based digital surface model (DSM), geographic information of GCPs in the study area must be determined using sensitive devices (i.e. TS and RTK-GPS) (Oniga et al., 2018). In this study, minimum horizontal and vertical accuracy of spatial data for GCPs were determined as  $\pm 0.05$  m using GNSS-GPS and TS. Total 20 GCPs were distributed over the forest road at a distance of 10 x 6 m (Figure 4).

### 2.4. SfM based Data Production

Seven main steps were taken in the design of a DSM using images from different locations. These steps generally involve digital camera calibration, the determination of image quality ('Image quality', which is an add-on feature of PhotoScan software, was used to remove images with an image quality index value lower than 0.5), creating photograph plane, positioning GCPs, and generation of SfM based spatial point clouds and other related data such as DSM and orthophoto. Manuel calibration was performed using "Agisoft Lens" add-on feature. In addition, PhotoScan software can automatically evaluate image quality. In this respect, images with an image quality index value lower than 0.5 were not included in the analysis (Agisoft, 2016).

Image processing steps described by Agisoft (2016) were followed in the study (Table 1). These steps are photograph alignment, building dense point clouds, building mesh model, building texture and building DSM using dense point clouds. After main tie points which align photographs had been generated, noisy points were manually removed, which resulted in a higher quality image for road surface models.

### 2.5. DSM Generated Using TS

A sensitive terrain model was produced thanks to TS in order to compare DSM data generated using SfM technique. Total of 69 GCPs including those obtained from the study area were collected from the road surface in millimeter sensitivity in order to obtain a terrain model. Point clouds generated using TS was used to produce raster surface model at a resolution of 0.02 m via "Inverse Distance Weight" (IDW) technique, which is an interpolation technique in Spatial Analyst, an add-on feature of ArcGIS (Childs, 2004; Esri, 2011). Then, the skidding road model, representing the road surface, was produced using 2-m buffer application beginning in the middle of the skidding road (right side and left side).

### 2.6. The Evaluation of DSM Generated Using SfM

DSMs were compared in terms of their visual and numerical aspects based on the sensitive measurements obtained from the study area. The correlation between DSMs collected from the study area using TS and generated using SfM technique was statistically analyzed. In addition, the correlation between SfM models and TS model as a statistical reference point was revealed. Finally, RMSE was metrically calculated for 275 randomly selected spatial points (Figure 5).

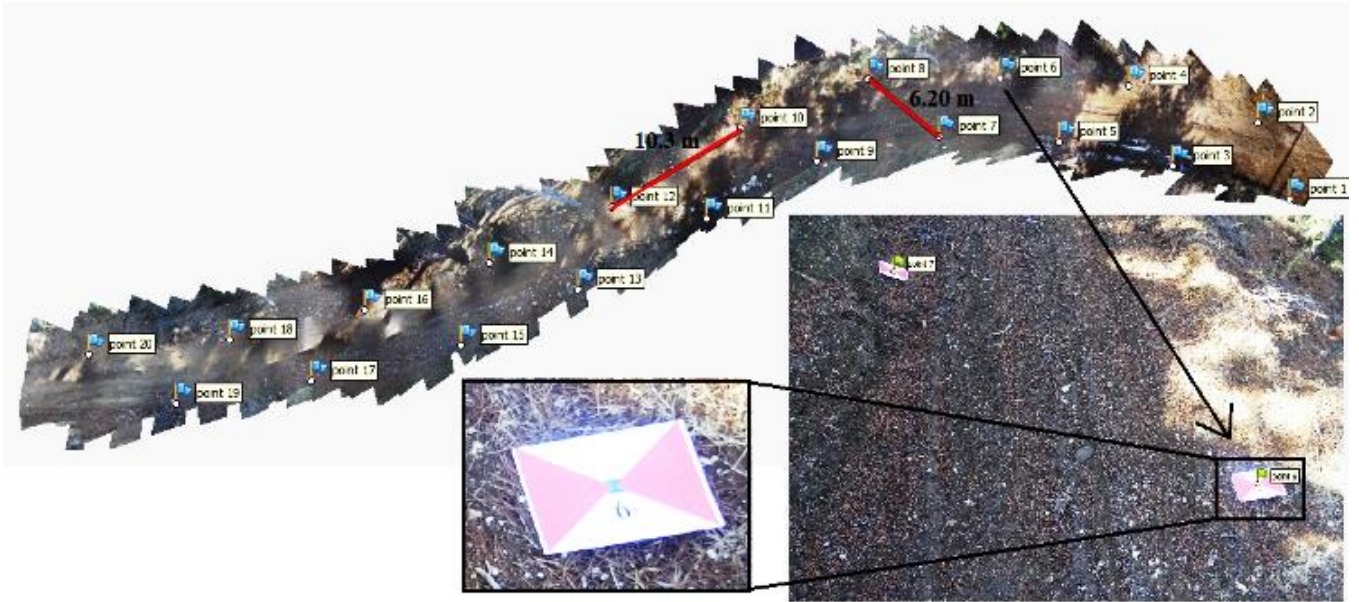


Figure 4. Distance between each GCPs and a general view

Table 1. Parameters used in six steps followed for SfM DSM generation

| <b>1-Align photos</b>  |                 | <b>2-Build dense cloud</b> |            | <b>3-Build mesh</b> |                 |
|------------------------|-----------------|----------------------------|------------|---------------------|-----------------|
| Accuracy               | Quality         | Quality                    | High       | Surface type        | Height field    |
| Pair selection         | Depth filtering | Depth filtering            | Aggressive | Source data         | Dense cloud     |
| Key point limit        | 40000           |                            |            | Face count          | High (18052588) |
| Tie point limit        | 4000            |                            |            | Interpolation       | Enabled         |
| <b>4-Build texture</b> |                 | <b>5-Build orthomosaic</b> |            | <b>6-Buil DEM</b>   |                 |
| Mapping source         | Orthophoto      | Surface                    | DEM        | Source data         | Dense cloud     |
| Blending mode          | Mosaic          | Blending mode              | Mosaic     | Interpolation       | Enabled         |
| Texture size           | 4096            |                            |            | Resolution (m/pix)  | 0.00248         |

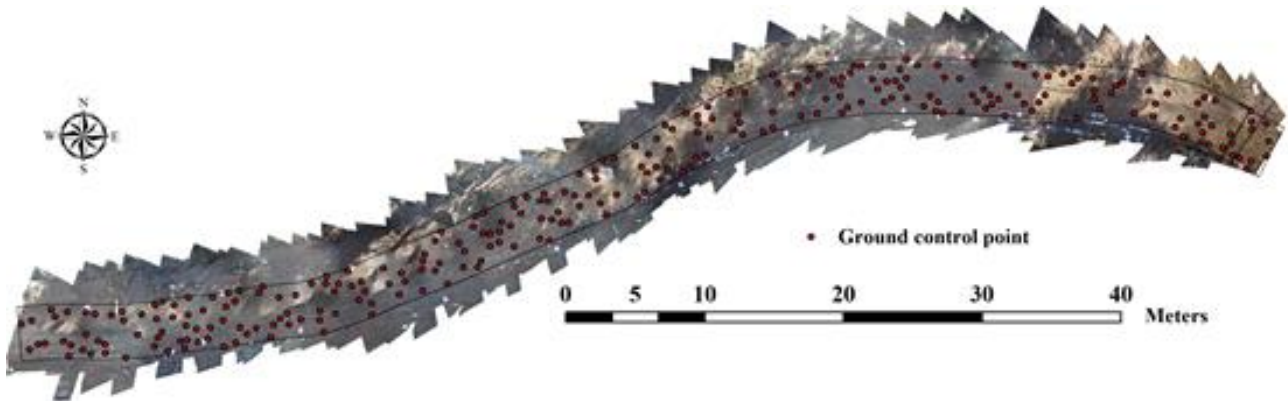


Figure 5. Spatial distribution of randomly selected points for the evaluation of elevation differences between the models

Two different surface models were generated for the study area, and surface difference models were designed in order to indicate the surface deformation. For this purpose, raster calculator (Equation 1), which is an add-on feature of ArcGIS, and surface analysis models within the “3D Analyst” add-on feature were used (Esri, 2011).

$$\text{Float} (“DSMSfM”- “DSMTS”) \quad (1)$$

Decimal numbers in DSM generated using SfM technique were converted to whole numbers to generate a raster (grid) data attribute table and calculate decimal volume. Additionally, a number of cutting, intersecting

and conversion processes were carried out to determine the study area in ArcGIS.

### 3. Results and Discussion

#### 3.1. SfM based DSM

Photo alignments were built in medium quality. A high quality and an aggressive filter were selected for dense point cloud generation (Table 1). Total of 97 images with an image quality index higher than 0.5 were included in the image processing. And, 95 out of 97 images were centered in the image alignment. Photoscan software identified 72.330 different tie points, and

90.262.944 spatial 3D points were generated in the dense point cloud generation process. After noisy spatial 3D points were manually removed, the number of main tie points and dense point clouds decreased to 68.087 and 87.690.758, respectively (Figure 6).

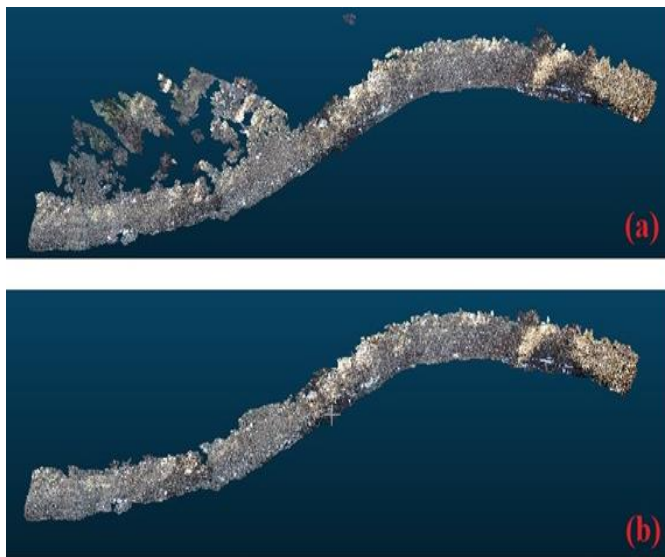


Figure 6. Tie points and dense point clouds in DSM generation (a) and the data obtained following the removal of noisy spatial 3D points (b)

After noisy spatial points had been removed, projection error was estimated as 1.72 pixel by PhotoScan software. The station elevation of the digital camera was calculated as 4.97 meters. In addition, a ground resolution of 1.21 mm/pixels was obtained following this process. The model was generated after SfMXY and SfMZ error values had been calculated 0.05 and 0.01 m, respectively. The data related to spatial errors identified using GCPs are given in Table 2.

Table 2. Errors of GCPs of SfM based model

| No    | XY error | Z error | Total error | Error |
|-------|----------|---------|-------------|-------|
| GCP1  | 0.023    | 0.000   | 0.023       | 0.270 |
| GCP2  | 0.047    | 0.008   | 0.047       | 0.115 |
| GCP3  | 0.014    | -0.016  | 0.022       | 0.050 |
| GCP4  | 0.033    | 0.003   | 0.033       | 0.206 |
| GCP5  | 0.020    | 0.004   | 0.020       | 0.087 |
| GCP6  | 0.009    | 0.000   | 0.009       | 0.053 |
| GCP7  | 0.008    | 0.001   | 0.008       | 0.069 |
| GCP8  | 0.019    | 0.002   | 0.019       | 0.049 |
| GCP9  | 0.004    | 0.001   | 0.005       | 0.068 |
| GCP10 | 0.012    | -0.024  | 0.027       | 0.041 |
| GCP11 | 0.025    | 0.021   | 0.032       | 0.058 |
| GCP12 | 0.030    | 0.012   | 0.032       | 0.051 |
| GCP13 | 0.013    | -0.014  | 0.019       | 0.068 |
| GCP14 | 0.034    | 0.007   | 0.035       | 0.150 |
| GCP15 | 0.035    | -0.014  | 0.038       | 0.034 |
| GCP16 | 0.035    | 0.009   | 0.037       | 0.035 |
| GCP17 | 0.094    | 0.003   | 0.094       | 0.063 |
| GCP18 | 0.119    | 0.008   | 0.119       | 0.095 |
| GCP19 | 0.112    | -0.009  | 0.112       | 0.042 |
| GCP20 | 0.009    | -0.002  | 0.009       | 0.195 |
| Total | 0.048    | 0.010   | 0.049       | 0.107 |

The resolution of SfM based DSM was calculated as 2.43 mm/pixels. In addition, spatial point density was measured as 169782 points per square meter (Figure 7). Photograph alignment was the most time-consuming process for DSM generation. The time elapsed for each process is summarized in Table 3.

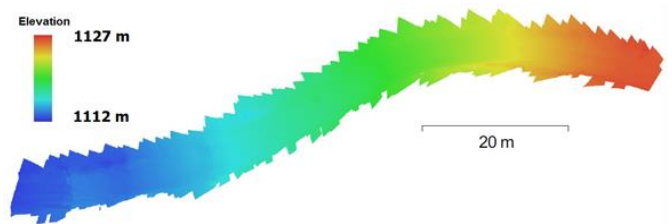


Figure 7. SfM based DSM generated using PhotoScan

Table 3. Image processing times elapsed for SfM based DSM

| Process           | Time        |
|-------------------|-------------|
| Photo alignment   | 15 min 34 s |
| Dense point cloud | 15 min 20 s |
| Mesh model        | 6 min 41 s  |
| Texture           | 11 min 20 s |
| Total             | 48 min 55 s |

### 3.2. DSM Generated Using TS Measurements

Five fixed stations were installed for 69 spatial measurement points in the study area. The measurements of spatial points were completed in nearly 45 minutes. Spatial point values were used to generate raster surface model at a resolution of 0.02 m via “Inverse Distance Weight” (IDW) technique, which is an add-on feature of ArcGIS software (Childs, 2004; Esri, 2011). The generated terrain model was used to produce road platform (Figure 8). Thanks to GCPs measured in the study area, minimum and maximum elevation differences of the model generated using IDW were estimated as 1126.42 and 1112.64 meters, respectively. In addition, minimum and maximum elevation differences of the road platform in the generated model were calculated as 1126.39 and 1112.64 m, respectively.

### 3.3. The Comparison of DSM Data

Both models generated using TS and SfM technique were visually compared, and it was observed that the surface model using SfM technique revealed morphological deformations on the road surface in more realistically compared with TS (Figure 9). Maximum and minimum elevation values of the digital surface model generated using TS were calculated as 1126.39 and 1112.64 meters, respectively. On the other hand, maximum and minimum elevation values of the model generated using SfM were calculated as 1126.41 and 1112.36 meters, respectively (Figure 7; Figure 8; Figure 9). The statistical data of the randomly selected sampling points are given in Table 4.

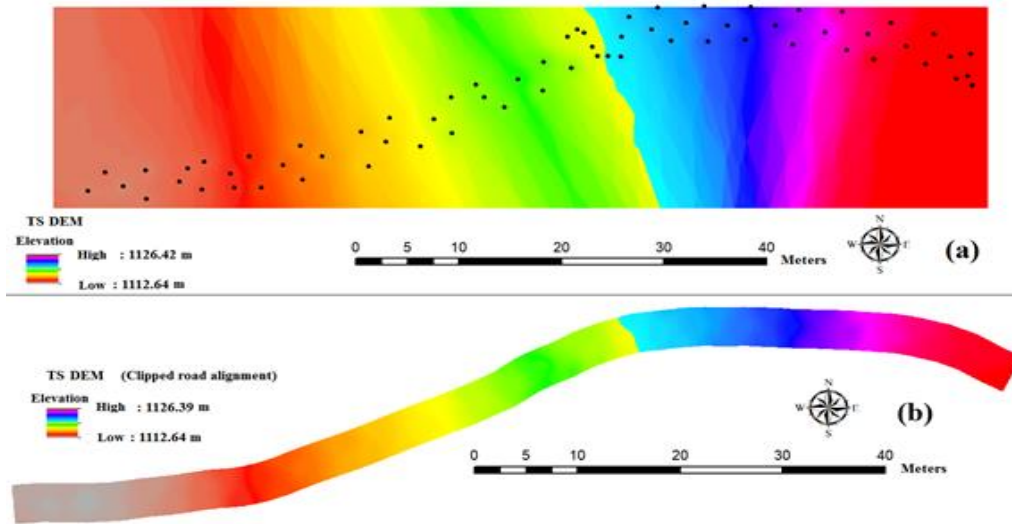


Figure 8. The model produced using spatial points measured via TS (a) and the road platform obtained from the model (b)

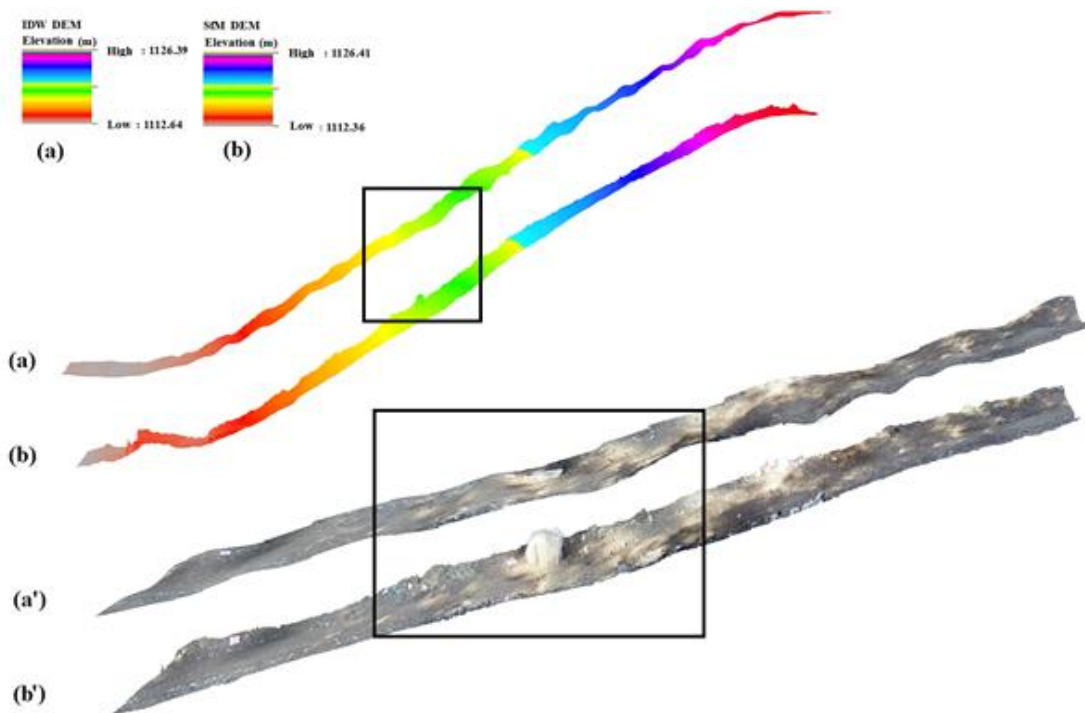


Figure 9. The comparison of DSM images generated using IDW technique (a) and SfM technique (b) (The rock fallen on the road surface obtained from IDW (a') and SfM (b') models)

Table 4. The statistical elevation data of randomly selected sampling points and reference points

|     | N   | Min.    | Max.    | Mean     | SD    | Var.   |
|-----|-----|---------|---------|----------|-------|--------|
| TS  | 275 | 1112.71 | 1126.34 | 1118.527 | 4.497 | 20.226 |
| SfM | 275 | 1112.42 | 1126.36 | 1118.574 | 4.428 | 19.607 |

RMSEZ value was calculated as 0.218 m for SfM based model. Unlike previous studies which measured at a sensitivity of 2 centimeters (Gonçalves et al., 2016; Hruza et al., 2016), this error rate in the present study may be attributed to the fact that a new road was used as a reference point. In other words, the error rate was found high because the road was built prior to the hauling operation. It was understood from Pearson's correlation analysis that there was a highly positive significant correlation between two models ( $p = 0.00$ ,  $p < 0.01$ ). In

addition, it was observed that various factors such as the locations of randomly selected GCPs, wheel ruts in the SfM based model, surface gullies resulting from water flow, and stones and rocks fallen on the road surface caused an elevation difference between the reference DSM and SfM DSM.

Volumetric differences between deformation models using SfM and TS were also analyzed. Accumulation on the road surface in the study area was calculated as  $0.035 \text{ m}^3$  per square meter. The road surface deformation per square meter was calculated  $-0.041 \text{ m}^3$  (wheel ruts and gullies), while the accumulation on the road surface per square meter was calculated as  $0.076 \text{ m}^3$ . Furthermore, volumetric calculations regarding the deformations in the surface model generated using PhotoScan were also performed (Figure 10).

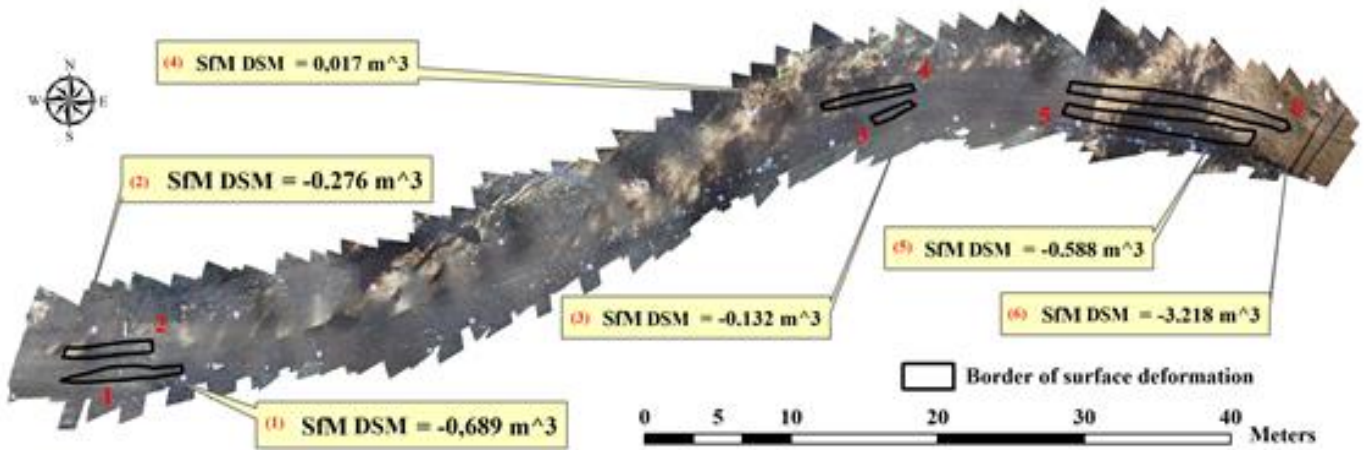


Figure 10. Volumetric estimations of gullies resulting from wheel ruts and wears on the road surface using SfM based DSM

It was understood in the present study that tractor wheel ruts caused a significant deformation on the surfaces with a lower slope. On the other hand, their impact was less significant on the surfaces with a higher slope. When it comes to road surfaces with a slope rate of 6-8%, gullies and wears were observed due to the hydrologic impact. It can be stated that surface deformations occurred on the whole skidding road which was not used and maintained following skidding operations. It was found out that surface deformation rates as a result of accumulation and abrasion did not significantly differ (Table 5).

Table 5. Deformation ratios on the road surface following the comparison of SfM and TS models

|          | Stable (%) | Accumulation (%) | Abrasion (%) | Total |
|----------|------------|------------------|--------------|-------|
| SfM – TS | 0.165      | 48.642           | 51.191       | 100   |

The minimum and maximum losses occurring as a result of surface change/deformation calculated using SfM were found as  $-0,022 \text{ m}^3$  and  $0.015 \text{ m}^3$ ,

respectively. The surface deformation map with a high resolution (0.242 cm) is shown in Figure 11. It was demonstrated that the accumulation of various materials such as soil, stones and harvesting residuals gradually increased as the elevation increased towards the western direction.

Although SfM method used in the present study offers a cost-efficient alternative for forest engineering data, it requires high-capacity image processing devices. However, it helps design sensitive road surface deformation models, and may be improved if it is supported by soil measurement data (Cambi et al., 2018). Similar studies which may pave the way for further modelling studies should benefit from other variables such as geometrical structure of the road and other external factors such as precipitation and tree species. Thus, it will be possible to determine the duration for an effective use of forest roads after their surface deformations resulting from the impact of natural factors and vehicle traffic are analyzed (Akgül et al., 2019).

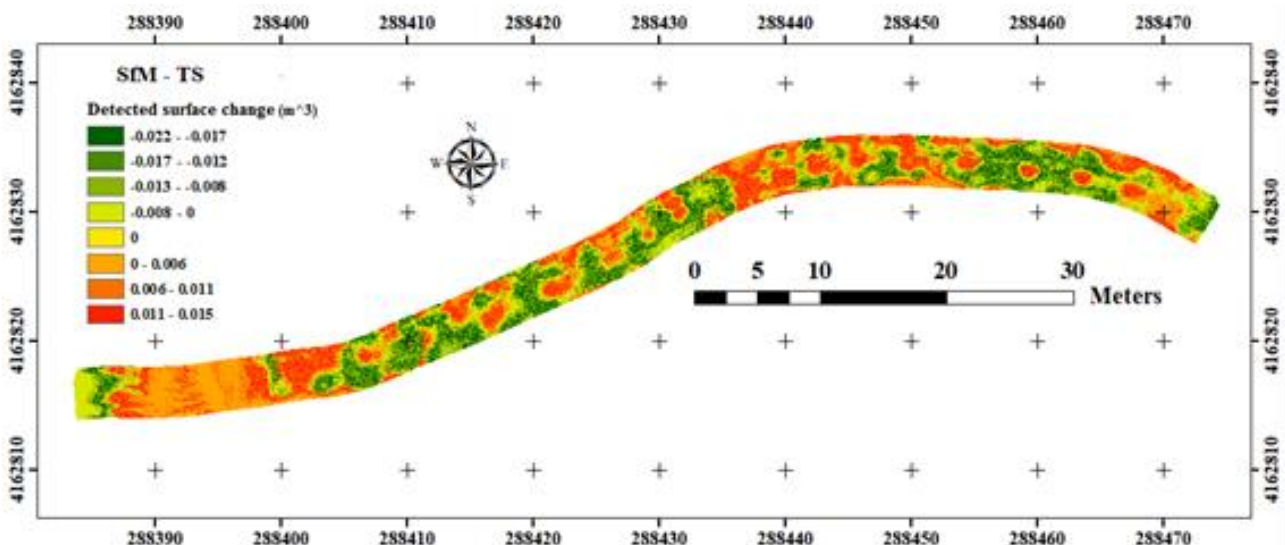


Figure 11. Volume map of road surface deformation and change calculated using the SfM - TS

Besides, maintenance and repair costs can be estimated beforehand, which will help to calculate approximate costs more realistically. For instance, forest engineers will determine the location which requires improvement works or low-cost hydrological structures such as culverts and increase the service life of problematic road surfaces by removing natural (harvesting residuals) and artificial (gravel etc.) materials. It was thus concluded that SfM based DSM could be used as a semi-automatic technique to determine temporal surface deformations on any forest road within the framework of forest construction and transport (Garbowski and Gajewski, 2017).

#### 4. Conclusion

The present study focused on the use of SfM technique in the evaluation of forest road surface deformation. This study was conducted as a short-term analysis, and two different models of temporal deformation were generated based on the measurements in different time periods. As a result, structural deformations occurring on the new skidding road during and following forestry operations were estimated. After the skidding road was closed to traffic following harvesting operations, it was observed that surface deformations (gullies and wheel ruts) and material accumulations (rocks, stones, soil and harvesting residuals) occurred on the skidding road within 6 months. Surface deformation were estimated on a road surface of 0.61 m<sup>3</sup> depending on the depth and width of tractor wheel ruts. In addition, a surface wear and gullies of 3.94 m<sup>3</sup> was estimated on the road due to hydrologic impact. The results indicated that the road was subject to a natural surface deformation of 99% following whole-tree skidding operation. It was also observed that material accumulation on the road surface exceeded abrasive factors such as gullies, wears and slumps. The findings of the present study indicated that SfM technique could offer acceptable and promising alternative compared with other high cost methods.

#### Acknowledgements

The present study includes data from MSc thesis titled “Using photogrammetric approach for assessment of forest road surface deformation due to forest transportation” (Thesis number: 547721) by Seçkin Şireli at Kahramanmaraş Sütçü İmam University, Graduate School of Science, Department of Forest Engineering, Kahramanmaraş, Turkey.

#### References

- Agisoft, 2016. Agisoft PhotoScan User Manual Professional Edition, Version 1.2. ed. St. Petersburg, Russia.
- Ahmed, M., Haas, C.T., Haas, R., 2011. Toward low-cost 3D automatic pavement distress surveying: the close range photogrammetry approach. *Canadian Journal of Civil Engineering*, 38(12): 1301-1313.
- Akay, A.E., Yuksel, A., Reis, M., Tutus, A., 2007. The impacts of ground-based logging equipment on forest soil. *Polish Journal of Environmental Studies*, 16(3):371.
- Akay, A.O., 2016. Determination of temporal changes on forest road pavement with terrestrial laser scanner. Master Thesis, Istanbul University, Institute of Graduate Studies in Science and Engineering, Department of Forest Engineering. Istanbul. 58 p.
- Akay, A.O., Akgul, M., Demir, M., 2018. Determination of temporal changes on forest road pavement with terrestrial laser scanner. *Fresenius Environmental Bulletin*, 27(3):1437-1448.
- Akgul, M., Akburak, S., Yurtseven, H., Akay, A. O., Cigizoglu, H. K., Demir, M., Ozturk, T., Eksi, M., 2019. Potential impacts of weather and traffic conditions on road surface performance in terms of forest operations continuity. *Applied Ecology and Environmental Research*, 17(2): 2533-2550.
- Akgul, M., Yurtseven, H., Akburak, S., Demir, M., Cigizoglu, H.K., Ozturk, T., Eksi, M., Akay, A.O., 2017. Short term monitoring of forest road pavement degradation using terrestrial laser scanning. *Measurement*, 103: 283-293.
- Arıca, B., Acar, H.H., 2008. The modeling of filling and construction impact areas in building forest roads by using quickbird satellite image. *Kastamonu Univ., Journal of Forestry Faculty*, 8(2): 144-156.
- Arıca, B., Genç, Ç.O., 2018. Technical efficiency evaluation of forest roads with respect to topographical factors and soil characteristics. *Baltic Forestry*, 24(1):123-130.
- Cambi, M., Giannetti, F., Bottalico, F., Travaglini, D., Nordfjell, T., Chirici, G., Marchi, E., 2018. Estimating machine impact on strip roads via close-range photogrammetry and soil parameters: a case study in central Italy. *iForest-Biogeosciences and Forestry*, 11(1): 148.
- Childs, C., 2004. Interpolating surfaces in ArcGIS spatial analyst. ArcUser, July-September, 32-35 p. <https://www.esri.com/news/arcuser/0704/files/interpolating.pdf>. (Accessed: 01 September 2018).
- Çankal, Ş.D., 2016. Assessment of roads within forested areas for visual quality aspect. Master Thesis. BTU, Institute of Graduate Studies in Science, Department of Forest Engineering. 41 p.
- Demir, M., 2012. Interactions of forest road, forest harvesting and forest ecosystems. *Forest Ecosystems—More than Just Trees* Dr Juan A Blanco. ISBN 953-978
- Erdaş, O., Acar, H.H., Eker, M., 2014. Transportation techniques of forest products, Karadeniz Technical University Press, K.T.U. No: 233. F.E. No: 39, Trabzon, ISBN: 978-975-6983-75-1. [Turkish]
- Eroglu, H., Acar, H., Eker, M., 2003. An evaluation of the forest road superstructure in Turkey, in: 12th World Forestry Congress. Congress Proceedings, Quebec, 4–6.

- Esri, R., 2011. ArcGIS desktop: release 10. Environmental Systems Research Institute, CA.
- Garbowski, T., Gajewski, T., 2017. Semi-automatic inspection tool of pavement condition from three-dimensional profile scans. *Procedia Engineering*, 172: 310-318.
- Gonçalves, J.A., Moutinho, O.F., Rodrigues, A.C., 2016. Pole photogrammetry with an action camera for fast and accurate surface mapping. *International Archives of the Photogrammetry, Remote Sensing & Spatial Information Sciences*. 41 p.
- Hrůza, P., Mikita, T., Tyagur, N., Krejza, Z., Cibulka, M., Procházková, A., Patočka, Z., 2018. Detecting forest road wearing course damage using different methods of remote sensing. *Remote Sensing*, 10(4): 492.
- İnan, M., Öztürk, T., 2016. Investigations of using the low cost close-range photogrammetry for forest roads conditions. 6<sup>th</sup> Remote Sensing-GIS Symposium, 5-7 October 2016, Adana, Turkey. pp. 254-258.
- Micheletti, N., Chandler, J.H. Lane, S.N., 2015. Structure from motion (SfM) photogrammetry. IN: Clarke, L.E. and Niell, J.M. (Eds.) *Geomorphological Techniques (Online Edition)*. London: British Society for Geomorphology. ISSN: 2047-0371, Chap. 2, Sec. 2.2.
- GDF, 2012. Forest Management Plan of Başkonuş, Forest Enterprise Chief (2012 – 2021). <https://www.ogm.gov.tr/ekutuphane/default.aspx> (Accessed: 12 March 2018) [Turkish]
- Oniga, V.E., Breaban, A.I., Stănescu, F., 2018. Determining the optimum number of ground control YKNs for obtaining high precision results based on UAS images. In *Multidisciplinary Digital Publishing Institute Proceedings* 2(7): 352.
- Öztürk, T., Sevgi O., Akay A.E., 2017. Impact assessment of log skidding on soil condition of skid roads during ground-based logging in a plantation forest in Istanbul, Turkey, *Bosque*, 38: 41-46.
- Pierzchała, M., Talbot, B., Astrup, R., 2016. Measuring wheel ruts with close-range photogrammetry. *Forestry: An International Journal of Forest Research*, 89(4): 383-391.
- Schnebele, E., Tanyu, B.F., Cervone, G., Waters, N., 2015. Review of remote sensing methodologies for pavement management and assessment. *European Transport Research Review*, 7(2): 7.
- Seki, M., Tiryakioğlu, İ., Uysal, M., 2017. Comparison of volumes done with different data collection methods. *Journal of Geomatics*, 2(2): 106-111.
- Şireli, S., 2019. Using photogrammetric approach for assessment of forest road surface deformation due to forest transportation. Master Thesis, Kahramanmaraş Sütçü İmam University, Institute of Graduate Studies in Science, Department of Forest Engineering, Kahramanmaraş. 82 p.
- Ünver, S. 2013. Determination of quality classes of forest roads by the point method: karanlıkdere sample. *Kastamonu Univ., Journal of Forestry Faculty* 13(2): 211-219. [Turkish]
- Worrell, R., Hampson, A., 1997. The influence of some forest operations on the sustainable management of forest soils—a review. *Forestry: An International Journal of Forest Research*, 70(1): 61-85.
- Yurtseven, H., Akgul, M., Akay, A.O., Akburak, S., Cigizoglu, H.K., Demir, M., Ozturk, T., Eksi, M., 2019. High accuracy monitoring system to estimate forest road surface degradation on horizontal curves. *Environmental Monitoring and Assessment*, 191(1):32.
- Zhang, S., Lippitt, C. D., Bogus, S.M., Neville, P.R., 2016. Characterizing pavement surface distress conditions with hyper-Spatial resolution natural color aerial photography. *Remote Sens*, 8(5): 392.